A Novel Control Method Focusing on Reactive Power for A Dual Active Bridge Converter

Jun-ichi Itoh, Hayato Higa, Tsuyoshi Nagano
Department of Electronics and Information Engineering
Nagaoka University of Technology
Nagaoka, Niigata, Japan
itoh@vos.nagaokaut.ac.jp, hhiga@stn.nagaokaut.ac.jp, ngn244@stn.nagaokaut.ac.jp

Abstract— This paper proposes a reactive current control method focusing on a copper loss reduction for a dual active bridge DC-DC converter. The proposed method controls the reactive current using the fundamental wave model of the primary and secondary voltages in the dual active bridge DC-DC converter. However, the total power factor reduced by the harmonic component of the output voltage of the each inverter in light load region. In order to keep the high total power factor, the pulse frequency modulation (PFM) is introduced to the proposed method. From the experimental results which the inductor current, total power factor, and the efficiency with the PFM compared without the PFM. The total power factor is over 0.88 from the 40% to the rated power with the PFM. In addition, the reactive power is controlled by adjusted switching frequency in order to achieve the minimum loss of a DAB converter prototype. As results, the efficiency of the prototype is improved 10% at 100 W. Therefore, it is confirmed that the proposed method achieves the minimum current value for the output power. In addition, the switching loss can be reduced by zero voltage switching with the reactive current control. Thus, the high efficiency can be achieved in wide load region.

Keywords— Bi-directional isolated DC-DC converter; Reactive current control; Dual active bridge DC-DC converter

I. INTRODUCTION

Recently, energy storage systems such as a battery have attracted for electric vehicles and power grid systems. Requirements of an energy storage system are a charge and discharge of a battery and safety in the emergency. Therefore, the battery conversion system has to need the isolation and bi-directional operation. In order to achieve the bi-directional power transmission and isolation, a bi-directional isolated DC-DC converter is used as energy storage systems [1-4]. There is a dual active bridge (DAB) converter such as a bi-directional isolated DC-DC converter [5-10]. A DAB converter obtains high efficiency and power density because zero voltage switching (ZVS) is achieved by a resonance between a leakage inductance in the high frequency transformer and a parasitic capacitance of switching devices during dead-time period [4]. In addition, transfer power of the DAB converter is determined by impedance of a leakage inductance in the high frequency transformer and a phase difference between output voltages of each inverter. Thus, the higher power capability cannot be achieved by higher frequency but also transformer of reduced size. However, the copper loss and the conduction loss of the switching device are increased because the ratio of the reactive current is increased in light regions. Furthermore, the ZVS area of the DAB converter is limited due to fluctuation in voltage such as a battery. These general approaches construct the switching pattern focusing on the achievement of ZVS in order to reduce the switching loss [5-7]. On the other hand, there are different approaches to decide pulse pattern in the DAB converter, which is focusing on the current reduction [8-12]. Especially, the copper loss of the transformer and conduction loss of semiconductors are higher than the switching loss depending on high power applications. Similarly, there is the approach that the switching frequency is increased with increment of the transfer power in term of the current reduction at rated power [7].This method has drawback that the reactive current cannot be reduced at light road. In addition, the operation area of the DAB converter is narrow because the transfer power is determined by impedance of the leakage inductance in the high frequency transformer. In the case which the voltage has a fluctuation such as a battery, the minimum loss of the DAB converter cannot be achieved in all load region.

This paper proposes a reactive current control method for a DAB converter in order to reduce the copper and the conduction loss. The proposed method controls active current and reactive current based on the secondary side voltage. The current is controlled to unity power factor against the secondary side voltage keeping ZVS conditions. In order to achieve the high total power factor, the pulse frequency modulation (PFM) is applied to the proposed method. In the proposed method, the ratio of the reactive current in all load region can be kept by increasing the switching frequency with decrease of the transfer power. As a result, the transformer current can be minimized by the proposed control. In addition, the high efficiency is achieved in wide load range by controlling the switching frequency according to the active current. This paper is organized as follows; at first, the proposed method which controls active current and reactive current based on the secondary side voltage is introduced. Secondary, the experimental waveforms when the proposed method with or without PFM are applied to the DAB converter are demonstrated. Next, the total power factors and the inductor currents when the proposed method with or without PFM are applied to the DAB converter are evaluated from the experimental results. In addition, it is confirmed that the ZVS is achieved and the ZVS area is extended by the reactive

978-1-4799-6768-1/14/$31.00 ©2014 IEEE

current control with PFM. As a result, the efficiency is improved by the proposed method with the PFM. It is clarified that the high total power factor is achieved in wide load region by the proposed method.

II. CONTROL STRATEGY

Fig. 1 shows a configuration of a bi-directional isolated DC-DC converter using DAB converter. This converter consists of a high frequency transformer and two voltage source inverters with H-bridge topology.

Fig. 2 shows a pulse pattern of the DAB converter in Fig. 1. In the DAB converter, output voltage waveforms of the each inverter are three-level voltage including the zero voltage periods or square waveform. The transfer power is determined by a phase difference δ between the primary output voltage v_1 and the secondary output voltage v_2, an impedance of the leakage inductance of the transformer [7]. In the dead-time period of each inverter, the ZVS operation is achieved by a resonance between a parasitic capacitance in the switching devices and the leakage inductance in the high frequency transformer.

Fig. 3 shows the ideal equivalent circuit of the DAB converter. In Fig. 3, this model consists of the square waveform or three-level waveform voltage sources and the leakage inductance of the high frequency transformer. In this section, the excitation inductance of the transformer is neglected because the exciting current is much smaller than the load current.

Fig. 4 shows an equivalent circuit model which is represented by the fundamental components of the primary side and the secondary side voltage of the DAB converter [11]. This model consists of the leakage inductance L and two sinusoidal voltage sources which have the fundamental component of the square waveform or the three-level waveform including the zero voltage periods. The proposed method considers the fundamental component

Fig. 5 shows the phaser diagram of the proposed control method which mentions relationship among the each voltages and the current of the high frequency transformer on the complex plane when the primary voltage is divided into the real part and the imaginary part based on the secondary voltage $\boldsymbol{V_2}$. That is, the active current and the reactive current are defined by not the primary voltage but the secondary voltage. In Fig. 4, $V_{1\alpha}$ is the real part of the primary voltage, $V_{1\beta}$ is the imaginary part of the primary voltage, $V_{2\alpha}$ is the real part of the secondary voltage, $\boldsymbol{V_L}$, $\boldsymbol{I_L}$ are the inductor voltage and the inductor current, δ is the phase difference between the primary voltage and the secondary voltage, $\boldsymbol{S}$ is an apparent power which is considered by the fundamental component voltage and current. The primary voltage $\boldsymbol{V_1}$ and the secondary voltage $\boldsymbol{V_2}$ are expressed by (1) and (2).

$$\boldsymbol{V}_1 = V_{1\alpha} + jV_{1\beta} \tag{1}$$

$$\boldsymbol{V_2} = V_{2\alpha} \tag{2}$$

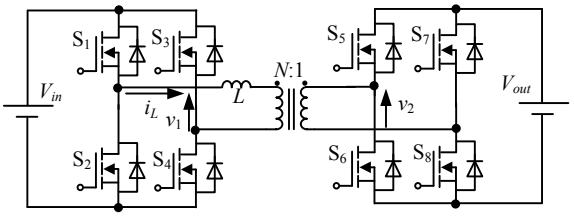

Fig. 1. A configuration of A DAB converter.

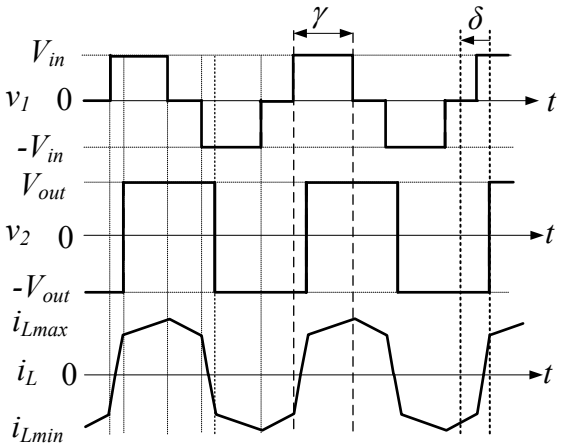

Fig. 2. Switching pattern of the DAB converter.

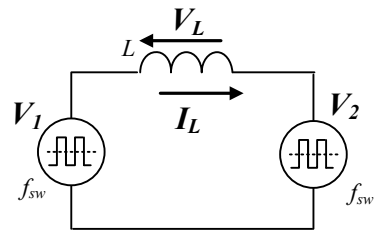

Fig. 3. Ideal equivalent circuit of DAB converter.

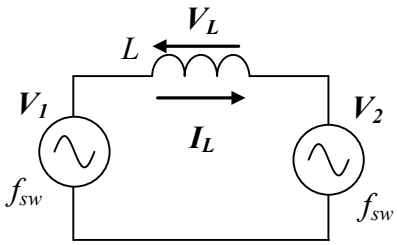

Fig. 4. Fundamental wave model of DAB converter.

The inductor current $\boldsymbol{I_L}$ is determined by the primary voltage, the secondary voltage, the switching frequency and the leakage inductance in the high frequency transformer.

$$\boldsymbol{I_L} = \frac{\boldsymbol{V_1} - \boldsymbol{V_2}}{j2\pi f_{sw}L} = I_{L\alpha} + jI_{L\beta} = \frac{V_{1\beta}}{2\pi f_{sw}L} + j\frac{(V_{2\alpha} - V_{1\alpha})}{2\pi f_{sw}L} \tag{3}$$

where, $I_{L\alpha}$ is the active current, $I_{L\beta}$ is the reactive current based on the secondary voltage, $2\pi f_{sw}L$ is the impedance of the transformer leakage inductance. From (2) and (3), the apparent power is given by (4).

$$\boldsymbol{S} = \boldsymbol{V_2 I_L} = P_{DC} + jQ = \frac{V_{1\beta} V_{2\alpha}}{2\pi f_{sw} L} + j\frac{V_{2\alpha}(V_{1\alpha} - V_{2\alpha})}{2\pi f_{sw} L} \quad (4)$$

where, the first term of (4) is the active power P_{DC}, that is the transmission power and the secondary term is the reactive power Q. In order to eliminate the reactive power, it is necessary that the real part of the primary side agrees with that of the secondary voltage. From (4), real part of the primary voltage is expressed by (5).

$$V_{1\alpha} = I_{L\beta}{}^{*} 2\pi f_{sw} L + V_{2\alpha} \quad (5)$$

where,. $I_{L\beta}{}^{*}$is the reactive current command. When the reactive current command is zero, the primary and the secondary voltage become equal. From (4), the imaginary part of the primary voltage is expressed by (6).

$$V_{1\beta} = 2\pi f_{sw} L \frac{P_{DC}{}^{*}}{V_{2\alpha}} \quad (6)$$

where,. $P_{DC}{}^{*}$ is the active power command. From (5) and (6), in order to control the reactive current, the primary voltage of transformer must be higher than the secondary voltage of transformer. Therefore, the primary voltage or the secondary voltage should be controlled. A phase difference δ between the primary and the secondary voltage of transformer is given by (7).

$$\delta = \tan^{-1}\frac{V_{1\beta}}{V_{1\alpha}} \quad (7)$$

In the proposed method, a phase difference δ is determined by the real and imaginary part of the primary side voltage based on secondary side voltage. From (5) to (7), a phase difference δ is determined by the transfer power command and reactive current command. In order to control the reactive current of the DAB converter by the proposed method, it is necessary that the primary voltage is controlled in order to achieve the primary voltage command. The output voltage period γ is given by (8) when the output voltage of the primary inverter is three-level voltage including the zero voltage periods.

$$\gamma = 1 - \frac{2}{\pi}\cos^{-1}\left\{\frac{\pi\sqrt{2(V_{1\alpha}{}^2 + V_{1\beta}{}^2)}}{4V_{in}}\right\} \quad (8)$$

where, V_{in} is the input voltage. The amplitude of the primary side voltage can be controlled by the output voltage period γ. Thus, the primary voltage controlled can be achieved when the output voltage of the primary inverter is three-level operation. In light load region, the reactive current control of the fundamental component is not effective because the total power factor will be reduced by the harmonic component because a narrow pulse width is used. On the other hand, from

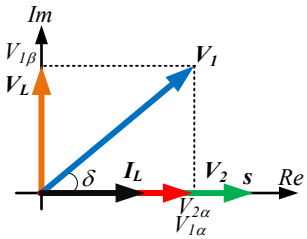

Fig. 5. Phaser diagram with voltages and the current of transformer with complex notation based on fundamental wave model.

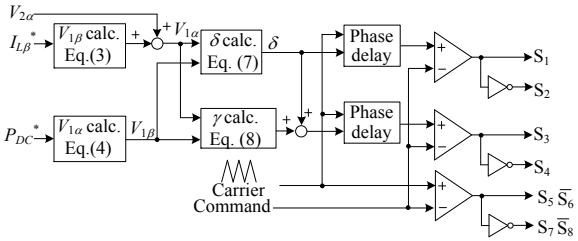

Fig. 6. Control diagrams for the proposed method.

TABLE I EXPERIMENTAL CONDITIONS

Input voltage	200V	Transformer turn ratio	1
Output voltage	100V	Leakage indactance	83μH
Rated power	700W	Dead-time	500ns
Carrier frequency with thePFM	32kHz-80kHz		
Carrier frequency without the PFM	32kHz		
MOS-FET	STW75NF-30		

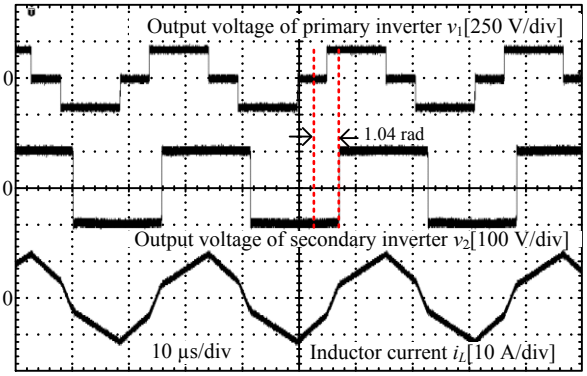

Fig. 7. Operation waveform at the rated power with proposed method applying the PFM and not applying the PFM (the switching frequency is 32 kHz.) .

(4), when the switching frequency is increased, the impedance of the leakage inductance in the high frequency transformer is increased. Then, the output power can be decreased by increasing the switching frequency while keeping on the value of $V_{1\alpha}$ and $V_{1\beta}$ because the impedance of the leakage inductances increases. As a result, the high total power factor operation is achieved in wide load region by controlling the switching frequency according to the load.

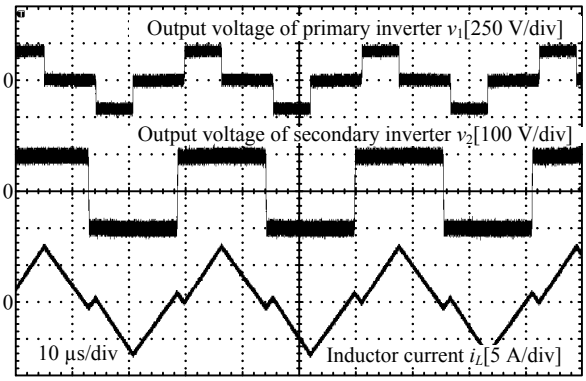

(a) The 44% rated power without the PFM (switching frequency is 32 kHz)

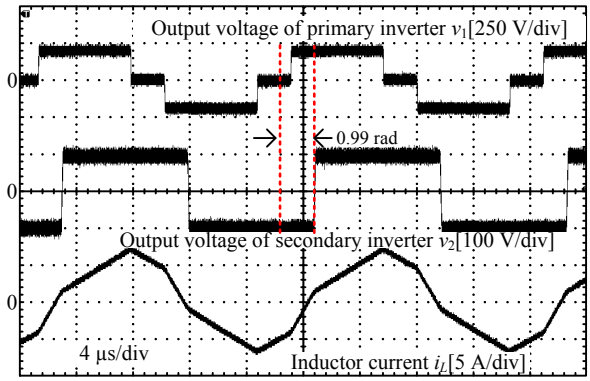

(c) The 44% rated power with the PFM (switching frequency is 64 kHz)

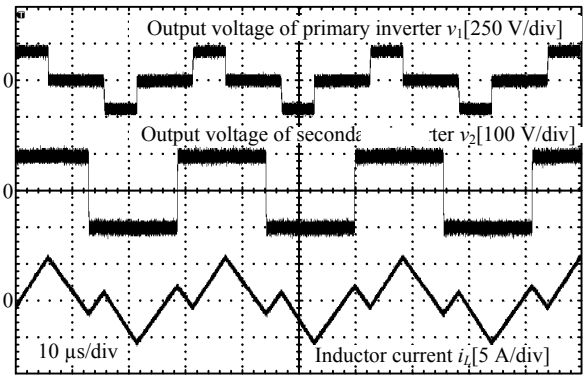

(b) The 26% rated power without the PFM (switching frequency is 32 kHz)

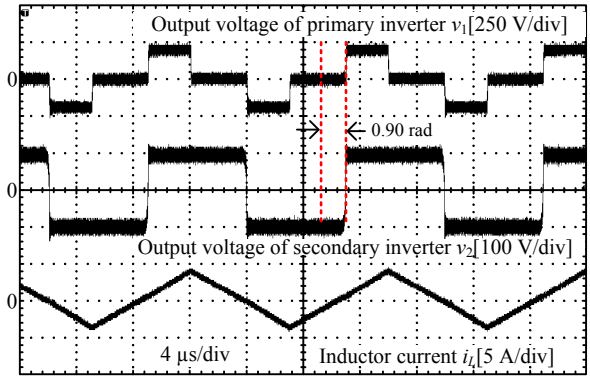

(d) The 26% rated power with the PFM (switching frequency is 72 kHz)

Fig. 8 Operation wave forms with the PFM or without the PFM. The error between the phase difference of the primary side and the secondary voltage at the 44% rated power and the 26% rated power.

Fig. 6 shows the control diagram of the proposed method. In order to achieve the reactive current control using (5) to (8), carriers of the primary and the secondary inverter are phase shifted. The phase shift amount of two carriers are determined by the phase difference δ and the output voltage periods γ of the three-level voltage including the zero voltage periods.

III. Experimental Results

In this section, the experimental results are demonstrated in order to evaluate the proposed method. In the experiment, the total power factor, the inductor current, the efficiency and the ZVS area are confirmed by the proposed method applied to the DAB converter prototype.

Table 1 shows the experimental conditions. In Table 1, STW75NF-30 of the MOS-FETs is selected. The on resistance of STW75NF-30 is 34 mΩ. The leakage inductance of transformer is 83 μH. However, the inductance is connected to the primary side of the transformer in order to achieve the leakage inductance of the transformer in Table 1. The switching frequency is 32 kHz with the PFM and without the PFM at the rated power because the value of the rated power is same with the PFM and without the PFM. Note that total power factor is determined by the inductor current and the secondary side voltage.

Fig. 7 shows the output voltages of the primary and the secondary inverter and the inductor current at the rated power with the PFM and without the PFM. In Fig. 7, the phase difference at the rated power between the output voltage of the primary and the secondary inverter is 1.04 rad. From inductor current and the secondary voltage waveform, the high total power factor is achieved because harmonic component of the inductor current is small.

Fig. 8(a) shows the operation waveform at the 44% rated power without the PFM and Fig. 8(b) shows the operation waveform at the 26% rated power without PFM. In Fig. 8(a), and Fig. 8(b), the transfer power can be changed by a phase difference between the primary voltage and the secondary voltage and the output voltage period as shown in (7). Fig. 8(c) shows the operation waveform at the 44% rated power with the PFM. The inductor current in Fig. 8(a) has more harmonic component than Fig. 8(c) owing to the short output voltage period γ which the primary voltage of Fig. 8(a) has. In same ways, the inductor current in Fig. 8(b) has more harmonic component than Fig. 8(d). Note that the output voltage period γ is adjusted in Fig. 8(d) because the maximum switching frequency is limited by the performance of the switching device. In addition, in Fig. 8(a), the phase difference at the 44% rated power with PFM is 0.99 rad. On the other hand, in Fig. 7, the phase difference at the rated power with PFM is 1.04 rad. The error between the phase difference at the rated power and the 44% rated power with the PFM is 4.8 % (i.e. the phase differences at the rated power and the 44% rated power are almost the same). Thus, the output power can be decreased while keeping on the value of $V_{1\alpha}$ and $V_{1\beta}$ by applying the PFM.

As a result, as mention below, the reactive current control can be achieved.

Fig. 9 shows the total power factor with the PFM and without the PFM. In the result without the PFM, the total power factor is 0.9 at rated power. However, the total power factor at light load is decreased. This is the reason that there are many harmonic components in inductor current owing to short output voltage period γ which the primary voltage has as shown in Fig. 8(a). On the other hand, the total power factor is over 0.88 from the 40% rated power to the rated power when the PFM is applied to the proposed method. This is because the reactive current control can be achieved in wide load region by keeping on the value of $V_{1\beta}$ and $V_{1\alpha}$ by applying the PFM. Thus, the reactive current is reduced in wide load region by the applying the PFM. However, the total power factor is decreased in the light load region. Because the maximum switching frequency is limited by the switching devices, the harmonic component of the primary voltage is increased by the output voltage period which is narrow width in the light load region.

Fig. 10 shows the gate signal and the terminal voltage of S_4 and S_8. Fig. 10(a) shows a result of the rated power and (b) shows a result of the 30 % rated power. In Fig. 10(a), the gate signals turn on after the drain to source voltage is dropped by 0 V due to resonance the parasitic capacitance of the MOS-FET and the leakage inductance of the transformer. Therefore, the ZVS of the primary inverter and the secondary inverter is achieved. However, in Fig. 10(b), the ZVS of the primary inverter and the secondary inverter is not achieved. This cause that the inductor current at the 30% rated power is smaller than achieving the ZVS. In order to achieve the ZVS in light load region, it is necessary to increase the reactive current using the proposed method with the PFM.

Fig.11 shows the inductor current and the ZVS area with the PFM, without the PFM and adjusted reactive current with PFM. In Fig. 11, the inductor current is reduced by 50% at 100 W because the total power factor in the light load regions is improved by applying the PFM. In addition, the ZVS area with the PFM is from the 40% rated power to the rated power. However, the hard switching is achieved below the 40% rated power. The ZVS in the light load region can be achieved by the reactive current control. On the other hand, the ZVS area without the PFM is below the 20% rated power. This cause is that inductor current when ZVS is not achieved is larger than when the ZVS is achieved due to the low total power factor below the 20% rated power. In order to achieve the ZVS in wide load region, the reactive current is controlled by adjusted the switching frequency. As a result, the ZVS region is extended for 20% than the result with the PFM. However, the inductor current is increased because the reactive current is increased in order to achieve the ZVS in wide load regions. That is, the minimum loss of the converter loss can be achieved when the reactive current is controlled by the ratio of the switching loss and the copper and conduction loss.

Fig. 12 shows the efficiency of the DAB converter prototype with the PFM, without the PFM and the adjusted reactive current with the PFM. In the experimental results, the reactive current is eliminated by the proposed method. The

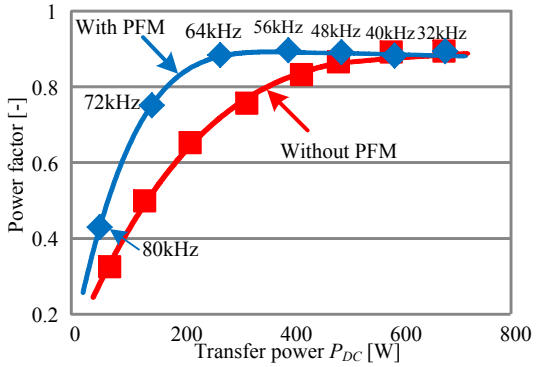

Fig. 9. The characteristics of total power factor with the PFM operation and without the PFM operation.

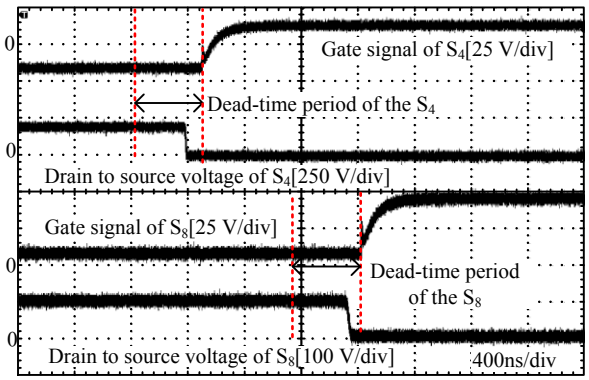

(a) Rated power

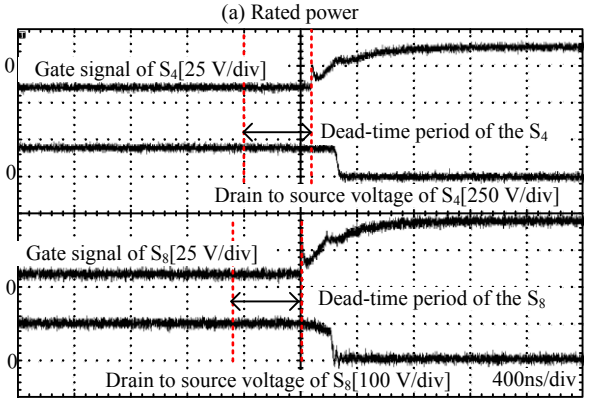

(b) 30% rated power

Fig. 10. The gate signal and terminal voltage between drain and source of the MOS-FET S_4, S_8 ZVS wave form at the 30% rated power.

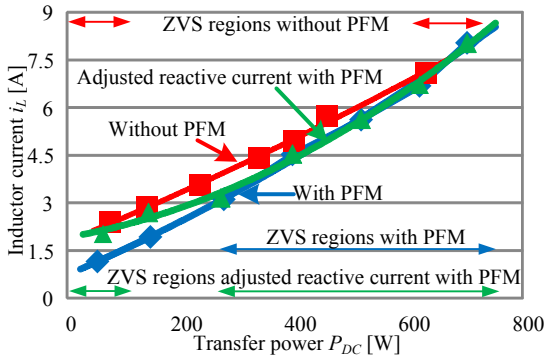

Fig. 11. The characteristics of inductor current and ZVS area with the PFM operation and without the PFM operation.

power flows from a primary side to the secondary side. In Fig. 12, the efficiency with the PFM from the 30% rated power to the 60% rated power is higher than without the PFM because the copper loss is reduced by applying the PFM. In addition, the switching loss without the PFM is increased by the hard switching from the 30% rated power to 70% the rated power. In the light load regions, the efficiency with the PFM is lower than without the PFM because the iron loss of the transformer and the switching loss are increased by the higher switching frequency. In order to improve the efficiency of the prototype with the PFM in the light load region, the reactive current is adjusted by decreasing the switching frequency. As a result, the efficiency of the prototype at 90 W is improved from 80.1% to 90.6% because the iron loss and the switching loss are decreased by the lower switching frequency. In the heavy load regions, the efficiency with the PFM is lower than without the PFM because the ZVS without PFM is achieved at 600 W. In addition, the copper loss with the PFM is increased by the skin effect. Therefore, it is necessary to optimize the switching frequency in order to achieve the minimum loss.

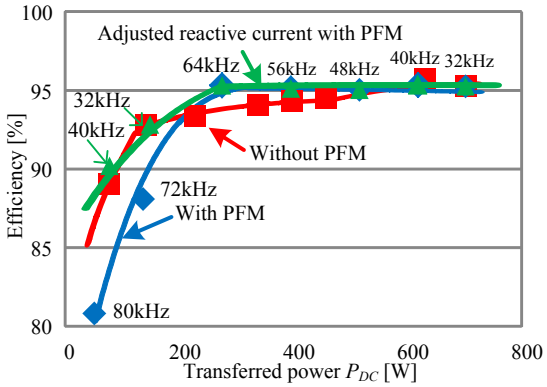

Fig. 12. The characteristics of the efficiency with the PFM, without the PFM and adjusted the reactive current with PFM.

IV. Conclusion

This paper proposed the reactive current control method for the DAB converter in order to reduce the copper loss. The voltage and the current of the transformer are discussed on complex plane using fundamental components. The experimental results are demonstrated in order to confirm the validity of the proposed control method. From experimental results, the total power factor with the PFM is over 0.88 from 40% to rated power. The inductor current is reduced by the 50% at 100 W with the PFM. In addition, the efficiency of converter at 100 W is improved from 80.9% to 90.1% by the adjusted reactive current. The ZVS area extended for 50% by adjusted the reactive current applied to the PFM. In the future work, relationship between the ZVS conditions and the component of the each voltage on the complex notation will be clarified. The theoretical formula is derived in order to achieve the minimum loss in all load region.

References

[1] R. T. Naayagi, Andrew J. Forsyth and R. Shuttleworth, "High-Power Bidirectional DC–DC Converter for Aerospace Applications", IEEE Transactions on Power Electronics, vol. 27, no. 1, pp. 4366-4379, Nov. 2012.

[2] Haihua Zhou and Ashwin M. Khambadkone, "Hybrid Modulation for Dual-Active-Bridge Bidirectional Converter With Extended Power Range for Ultracapacitor Application", IEEE Transactions on Power Electronics, vol. 45, no. 4, pp. 1434-1442, Jul. 2009.

[3] Manu Jain, M. Daniele and Praveen K. Jain, "A Bidirectional DC–DC Converter Topology for Low Power Application" IEEE Transactions on Power Electronics, vol. 15, no. 4, pp. 1434-1442, Jul. 2000.

[4] A. Jones, B. Smith and C. Maxwell, "Reactive Power Loss Optimization Method for Bi-directional Isolated DC-DC Converters", IEEE Transactions on Power Electronics, vol. 17, no. 1, pp. 45-55, Jan. 1995.

[5] G. G. Oggier, G. O. Garcia, A. R. Oliva, "Modulation strategy to operate the Dual Active Bridge DC-DC converter under Soft-Switching in the whole operating range", IEEE Trans. on Power Electronics, vol. 26, no. 4, pp. 1228-1236, Apr 2011.

[6] Giuseppe Guidi, Atsuo Kawamura, Yuji Sasaki and Tomofumi Imakubo "Dual Active Bridge Modulation with Complete Zero Voltage Switching Taking Resonant Transitions into Account" IEEE EPE 2011

[7] Shun Nagata ; Mika Takasaki ; Yukata Furukawa ; Toshiro Hirose ; Yoichi Ishizuka "A Static Characteristic Analysis of Proposed Bi-Directional Dual Active Bridge DC-DC Converter",IPEC2014, pp.2252-2260, May, 2014

[8] Amit Kumar Jain and Rajapandian Ayyanar "PWM Control of Dual Active Bridge: Comprehensive Analysis and Experimental Verification", IEEE Trans. on Power Electronics, vol. 26, no. 4, pp.1215-1227, Apr 2011.

[9] Biao Zhao, Qiang Song, Wenhua Liu and Weixin Sun "Current-Stress-Optimized Switching Strategy of Isolated Bidirectional DC-DC Converter With Dual-Phase-Shift Control", IEEE Trans. on Power Electronics, vol. 60, no. 10, pp.4458-4467, Oct 2013.

[10] Xiao-Fei He, Zhiliang Zhang, Yong-Yong Cai, Yan-Fei Liu"A Variable Switching Frequency Hybrid Control for ZVS Dual Active Bridge Converters to Achieve High Efficiency in Wide Load Range",APEC2014, pp.1095-1099, March, 2014

[11] Florian Krismer and Johann W. Kolar "Closed Form Solution for Minimum Conduction Loss Modulation of DAB Converters", IEEE Trans. on Power Electronics, vol. 27, no. 1 ,pp. 174-188 ,Jan 2012.

[12] Hua Bai and Chris Mi "Eliminate Reactive Power and Increase System Efficiency of Isolated Bidirectional Dual-Active Bridge DC-DC Converters Using Novel Dual-Phase-Shift Control" ,IEEE Trans. on Power Electronics, vol. 23, no. 6 ,pp. 2905-2914 ,Nov 2008.